

Thermodynamics of guest-induced structural transitions in hybrid organic–inorganic frameworks

François-Xavier Coudert^a, Marie Jeffroy^b, Alain H. Fuchs^c,
Anne Boutin^{b*}, Caroline Mellot-Draznieks^{a*}

March 24, 2021

^a Department of Chemistry, University College London,
20 Gordon Street, London, WC1H 0AJ, United Kingdom.

^b Laboratoire de Chimie Physique, CNRS and Univ. Paris-Sud,
F-91405 Orsay, France.

^c École nationale supérieure de chimie de Paris (Chimie ParisTech)
and Univ. Pierre et Marie Curie, F-75005 Paris, France.

* Corresponding authors: anne.boutin@lcp.u-psud.fr
and c.mellot-draznieks@ucl.ac.uk

Abstract

We provide a general thermodynamic framework for the understanding of guest-induced structural transitions in hybrid organic–inorganic materials. The method is based on the analysis of experimental adsorption isotherms. It allows the determination of the free energy differences between host structures involved in guest-induced transitions, especially hard to obtain experimentally. We discuss the general case of adsorption in flexible materials and show how a few key quantities, such as pore volumes and adsorption affinities, entirely determine the phenomenology of adsorption, including the occurrence of structural transitions. Based on adsorption thermodynamics, we then propose a taxonomy of guest-induced structural phase transitions and the corresponding isotherms. In particular, we derive generic conditions for observing a double structural transition upon adsorption, often resulting in a two-step isotherm. Finally, we show the wide applicability and the robustness of the model through three case studies of topical hybrid organic–inorganic frameworks: the hysteretic hydrogen adsorption in Co(1,4-benzenedipyrazolate), the guest-dependent gate-opening in Cu(4,4'-bipyridine)(2,5-dihydroxybenzoate)₂ and the CO₂-induced “breathing” of hybrid material MIL-53.

Introduction

Organic–inorganic framework materials display an extremely large range of crystal structures and host-guest properties, ranging from coordination polymers, porous metal–organic frameworks (MOFs), and extended inorganic hybrids.^{1–6} This makes them an important class of materials with potentially major impact in adsorption/separation technologies of strategic gas (H₂, CO₂ or CH₄).^{7–10} The combination of tunable porosity, the functionalization of the internal surface together with the structural flexibility of the host opens the way to an extremely rich host-guest chemistry, putting this class of materials in a unique position.

The distinctive chemistry that results from the flexibility of hybrid frameworks may be set against that of zeolites, that are characterized by a relatively limited framework flexibility and a high thermal stability due to the strength of the metal-oxygen bonds (Si–O bonds are among the strongest covalent bonds known), allowing their permanent porosity upon adsorption-desorption processes. By contrast, hybrid materials involve significantly weaker bonds (coordinative bonds, π – π staking, hydrogens bonds...) that are responsible for their intrinsic structural flexibility. Thus, one fascinating aspect of hybrid frameworks is the ability of a subclass of structures to behave in a remarkable guest-responsive fashion.^{11–14} As recently classified by Kitagawa et al.,^{13,14} such hybrid frameworks exhibit a variety of guest-induced structural phase transitions upon gas adsorption and desorption. They are typically reported to possess a bistable behavior controlled by an external stimulus such as gas pressure.

It is striking that a substantial number of experimental adsorption data collected on guest-responsive hybrid frameworks exhibit S-shape or step-wise adsorption isotherms, frequently assorted with hysteresis loops, this for a surprisingly large variety of polar and non polar sorbates (CO₂, CH₄, methanol, ethylene...).^{15–23} They include a recent example of hysteretic H₂ multi-step isotherms²⁴ that do not conform to any of the IUPAC isotherm types.²⁵ Despite the richness of the experimental data at hand on these systems, the fundamental thermodynamics that underlie these particularly complex {host-guest} systems is far from being understood today and its phenomenology remains to be developed. In this respect, we may put forward two strictly distinct situations.

For a number of hybrid frameworks, the S-shape of adsorption isotherms may be clearly attributed to the very large pore size of the material and the occurrence of strong sorbate-sorbate interactions reminiscent of the bulk, as shown in the case of CO₂ adsorption in a series of MOFs.^{26,27} In these situations, the shape of the isotherm does not arise from a phase transition of the host but from the details of the structural arrangement of the adsorbed phase, similarly to what occurs for a number of {zeolite, guest} systems (e.g. {silicalite-1/heptane}²⁸ and {AlPO₄-5/methane}²⁹). The phenomenology of such systems has been extensively studied and is appropriately described in the frame of the widely used Grand Canonical ensemble. We will not consider them further in this paper.

For another subclass of hybrids, which is the primary focus of this article, the presence of one or more steps in the isotherms has been attributed to guest-induced structural transitions of the host material. In this case, the phenomenology of gas adsorption is deemed to be far more complex, as shown experimentally by the great variety of isotherms profiles, hysteresis loops and types of phase transitions (classified as amorphous-to-crystal and crystal-to-crystal transformations).¹³ For example, among the most eye-catching guest-induced phase transitions of hybrids are the so-called “gate-opening” and “breathing” phenomena, attracting much attention due to their potential applications in sensing, gas separation or low pressure gas storage.^{23,30,31} “Gate-opening” typically involves an abrupt structural transition between a non-porous state and a porous crystalline host that

is induced by gas adsorption. It is characterized by highly guest-dependent “gate-opening” and “gate-closing” pressures (on the adsorption and desorption branches respectively).³¹ The “breathing” phenomenon includes two recent examples, MIL-53³² and MIL-88³³ transition metal terephthalates, that exhibit massive guest-induced crystal-to-crystal transformations. While MIL-88 exhibits a gradual cell expansion up to 200 % upon fluid adsorption,³⁴ an abrupt structural transition is observed in MIL-53 upon H₂O³² or CO₂ adsorption,³⁵ with a transition resulting in a ~38 % cell variation.

Despite a very rich experimental corpus of data, there is a dearth of systematic understanding of the thermodynamics of guest-responsive hybrid frameworks. Key questions remains to be answered such as, for example: (i) predicting the occurrence or absence of a guest-induced transition for a given {host, gas} system and predicting the resulting shape of the adsorption isotherm; (ii) elucidating the thermodynamics that underlie the guest-induced transition itself, including the relative stabilities of the two states; or (iii) identifying the key factors that drive the strong guest-dependence of the gate-opening processes.

One of the reasons that have hindered the systematic understanding of guest-responsive hybrid frameworks until now is that the thermodynamics of the two concomitant processes (host-guest interactions and the host structural transition) cannot be easily deconvoluted experimentally, even though it is generally agreed that the interplay between the host-guest interactions and the energetic cost of the structural transition governs the guest-induced structural transitions. The current approach in the field relies on the characterisation of the energetics of the adsorption, typically using calorimetric measurements which however do not distinguish the host and host-guest contributions. Alternatively, forcefield-based and DFT single point energy calculations^{36,37} have been used to elucidate the relative energetic contributions pertaining to the host and to the guest adsorption, although leaving the thermodynamic picture incomplete.

A complete description of the thermodynamics of guest-responsive frameworks can be obtained directly by carrying simulations of the fully flexible solid in presence of adsorbate, in the so-called osmotic ensemble. However, this method puts a demanding constraint on the forcefield development, as they are required to describe the full energy landscape of the host material, including the structural transition itself. Moreover, it is frequent with hybrid materials that the low crystallinity of phases involved in the transition hinders their structural determination from powder data, therefore eliminating the possibility of simulating their adsorption isotherms.

The present paper aims at rationalizing the thermodynamics of adsorption in flexible frameworks when guest-induced structural transitions of the host are involved. We first develop a thermodynamic description of the process of adsorption in flexible structures, and then devise a method to calculate the difference in free energy between the different structures involved in guest-induced structural transitions. This method relies on adsorption isotherms, which can be obtained experimentally. We then use the description developed to discuss the general case of type I adsorption in flexible materials, and we show that the thermodynamics of this process depends only on a few key quantities (pore volumes, adsorption affinities). This allows us to develop a taxonomy of the different behaviors that can be observed upon adsorption, and the resulting types of isotherm. Finally, we show the wide applicability and the robustness of our free energy calculation method by applying it to three topical guest-responsive hybrid materials: we study the hysteretic hydrogen adsorption in Co(1,4-benzenedipyrazolate), the guest-dependent gate-opening in Cu(4,4'-bipyridine)(2,5-dihydroxybenzoate)₂ and the CO₂-induced “breathing” of hybrid material MIL-53.

Thermodynamic potential in the osmotic ensemble

Expression of the thermodynamic potential of host-guest systems

We consider here the general process of adsorption of a fluid in a nanoporous material, where the host framework undergoes structural phase transitions induced by the adsorption of the fluid. It has been shown that this process is most appropriately described in the osmotic statistical ensemble,^{38–42} where the control parameters are the number of molecules of the host framework N_{host} , the chemical potential of the adsorbed fluid μ_{ads} , the mechanical constraint σ exerted on the system (which is simply here the external pressure P) and the temperature T . The osmotic ensemble in this formulation³⁹ is an extension of the grand canonical ensemble that accounts for the presence of a flexible host material with variable unit cell. Its thermodynamic potential Ω_{os} and configurational partition function Z_{os} are the following:⁴³

$$\Omega_{\text{os}} = U - TS - \mu_{\text{ads}}N_{\text{ads}} + PV \quad (1)$$

$$Z_{\text{os}} = \sum_V \sum_{N_{\text{ads}}} \sum_{\mathbf{q}} \exp[-\beta U(\mathbf{q}) + \beta \mu_{\text{ads}}N_{\text{ads}} - \beta PV] \quad (2)$$

where \mathbf{q} denotes the positions of the atoms of the system (host and adsorbate) and $\beta = 1/kT$ (k being the Boltzmann constant).

In order to study the relative stability of different phases of the host structure upon adsorption, our method relies on the factorization of the expressions above in two contributions, one characterizing the framework structures themselves (i.e. their free energy), the other describing the fluid adsorption in each solid phase involved in the transition. The summation over the positions \mathbf{q} of atoms in the system is thus split into a double summation over the coordinates of the material, \mathbf{q}_{host} , and coordinates of the atoms of the adsorbate, \mathbf{q}_{ads} . The total energy is the sum of the energy of the host, the energy of the adsorbed fluid and the host-adsorbate interactions:

$$U(\mathbf{q}) = U_{\text{host}}(\mathbf{q}_{\text{host}}) + U_{\text{ads}}(\mathbf{q}_{\text{ads}}) + U_{\text{host-ads}}(\mathbf{q}_{\text{ads}}, \mathbf{q}_{\text{host}}) \quad (3)$$

As our interest lies in the determination of adsorption-induced structural transitions of the host material, we make the assumption that while the fluid adsorption may favor one phase or another, each single structure is only marginally changed by the adsorption of fluid. This is translated into a mean field approximation by writing that the host-adsorbate interactions depend only on the average positions of the atoms (and unit cell vectors) of the material in a given phase i : $U_{\text{host-ads}}(\mathbf{q}_{\text{ads}}, \mathbf{q}_{\text{host}}) \simeq U_{\text{host-ads}}(\mathbf{q}_{\text{ads}}; \langle \mathbf{q}_{\text{host}} \rangle_i)$. Using this separation of variables, the configurational partition function can be written as a sum of configurational partition functions for each phase i of the solid: $Z_{\text{os}} = \sum_i Z_{\text{os}}^{(i)}$. The configurational partition function of any given phase i of the material is then given by:

$$Z_{\text{os}}^{(i)} = \left(\sum_{V \in i} \sum_{\mathbf{q}_{\text{host}} \in i} \exp[-\beta U_{\text{host}}(\mathbf{q}_{\text{host}}) - \beta PV] \right) \times \left(\sum_{N_{\text{ads}}} \sum_{\mathbf{q}_{\text{ads}}} \exp[-\beta U_{\text{ads}}(\mathbf{q}_{\text{ads}}) - \beta U_{\text{host-ads}}(\mathbf{q}_{\text{ads}}; \langle \mathbf{q}_{\text{host}} \rangle_i) + \beta \mu_{\text{ads}}N_{\text{ads}}] \right) \quad (4)$$

It is apparent that the first term is the configurational partition function (restricted to phase i) of the isolated host structure in the (N_{host}, P, T) ensemble, $Z_{\text{host}}^{(i)}$. The second term can be recognized as the grand canonical configurational partition function $Z_{\text{GC}}^{(i)}$ of the fluid in the external field created by the host framework considered as rigid. Thus, for each host phase (i), $Z_{\text{os}}^{(i)} = Z_{\text{host}}^{(i)} \times Z_{\text{GC}}^{(i)}$, can be written in terms of the thermodynamic potentials

for each ensemble: $\Omega_{\text{os}}^{(i)} = G_{\text{host}}^{(i)} + \Omega^{(i)}$, where Ω is the grand canonical potential for the adsorbate and G_{host} is the free enthalpy of the host material.

To express the grand canonical potential as a function of quantities directly available from experiments or simulations, we calculate it from its derivatives, using the fundamental relation involving the chemical potential μ_{ads} :^{44–46}

$$\left(\frac{\partial \Omega}{\partial \mu_{\text{ads}}} \right)_{V,T} = -N_{\text{ads}} \quad (5)$$

Integrating this equation and taking into account that $\Omega(P=0) = 0$, the grand canonical potential Ω can be rewritten as a function of pressure P rather than chemical potential μ_{ads} , as follows:

$$\Omega(P) = - \int_0^P N_{\text{ads}}(p) \left(\frac{\partial \mu}{\partial p} \right)_{T,N} dp \quad (6)$$

which can be simplified further by introducing the molar volume of the pure fluid, $V_m = (\partial \mu / \partial P)_{T,N}$:

$$\Omega(P) = - \int_0^P N_{\text{ads}}(p) V_m(p) dp \quad (7)$$

The free enthalpy of the host can also be written as a function of the free energy of the host at zero pressure, F_{host} : $G_{\text{host}} = G_{\text{host}}(P=0) + PV = F_{\text{host}} + PV$.

Finally, this leads to a complete expression of the osmotic potential which involves only three key parameters: the free energy of the solid phase, the adsorption isotherm of fluid inside that phase ($N_{\text{ads}}(T, P)$) and the molar volume of the pure fluid as a function of pressure:

$$\Omega_{\text{os}}(T, P) = F_{\text{host}}(T) + PV - \int_0^P N_{\text{ads}}(T, p) V_m(T, p) dp \quad (8)$$

Prediction of the free energy of phases involved in structural transitions

We now have an expression for the thermodynamic osmotic potential as a function of gas pressure for each solid phase. The comparison of Ω_{os} for each phase of the host allows us to determine the relative stability of the phases, the number of structural transitions that will take place and the pressure at which they occur. This requires the prior determination of the three quantities in Equation 8. The relative free energies of the empty solid phases ($F_{\text{host}}^{(i)}$) are especially difficult to evaluate both experimentally and by simulation methods. While relative energies between solid phases can be experimentally measured, for example by differential scanning calorimetry or the measurement of dissolution enthalpies,⁴⁷ or calculated using first-principles methods, the determination of relative *free energies* is a much harder task.

By contrast, the pressures at which guest-induced transitions happen are relatively easy to measure experimentally, either because they show up as steps on the adsorption isotherm, or by calorimetry (structural transitions often result in a sudden change in heat of adsorption) or even by *in situ* X-ray diffraction studies at different gas loadings. For that reason, we propose here a method to calculate the relative free energies of the empty solid phases ($F_{\text{host}}^{(i)}$) from the readily available experimental quantities that are the sorption isotherms and the phase transition pressure, using Equation 8.

The quantities involved in Equation 8 and that we need to calculate free energy differences are now the transition pressures, the adsorption isotherms for each isolated phase ($N_{\text{ads}}^{(i)}(P)$), the molar volume of the pure adsorbate as a function of pressure ($V_m(P)$) and the unit cell volume of each phase (V_i). That last two are rather straightforward to obtain: V_i is known from crystal structures determined by X-ray diffraction and $V_m(P)$ can

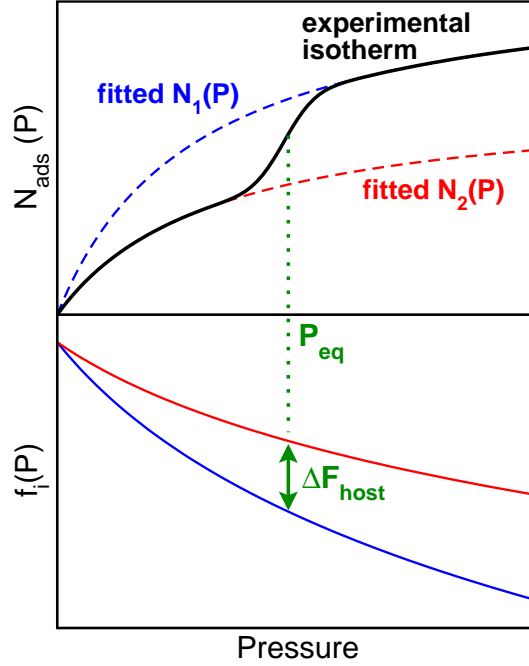


Figure 1: Schematic representation of the determination of free energy difference ΔF_{host} from an experimental adsorption isotherm (upper panel) by calculation of $f_i(P)$, the pressure-dependent part of the thermodynamic potential of the osmotic ensemble (lower panel).

be found tabulated for a large number of gases or alternatively approximated by the relation for an ideal gas, $V_m(P) = RT/P$. The pressures at which structural transitions occur may be determined from the experimental adsorption and desorption isotherms of the material or other methods described above. However, the “virtual” rigid-host isotherms $N_{\text{ads}}^{(i)}(P)$ related to each phase are harder to obtain experimentally: they correspond to each of the solid phases assuming the absence of transition over the whole range of pressures, so that only parts of these rigid-host isotherms are observed experimentally, as shown in Figure 1. To overcome this issue, we propose here to fit the distinct parts of a stepped isotherm to obtain full “rigid-host” isotherms needed for each of the phases. They correspond to the dashed lines in Figure 1. Alternatively, it is possible to use isotherms calculated from Grand-Canonical Monte Carlo simulations in each phase, with the host structure being considered rigid.⁴⁰

Let us illustrate here the method on an isotherm possessing a single step that corresponds to a guest-induced structural transition (Figure 1) between two phases labeled **1** and **2**, assuming **1** and **2** have been structurally characterized and have known unit cell volumes, V_1 and V_2 . From the step in the experimental isotherm, the pressure P_{eq} of the structural transition can be determined and the two parts of the isotherm (below and above the step) are fitted by Langmuir isotherms⁴⁸ (dashed lines on Figure 1). From the fitted isotherms $N_{\text{ads}}^{(i)}(P)$, we can now plot (Fig. 1, lower panel) the two functions $f_1(P)$ and $f_2(P)$ defined as:

$$f_i(P) = \Omega_{\text{os}}^{(i)}(P) - F_{\text{host}} = PV_i - \int_0^P N_{\text{ads}}^{(i)}(p) V_m(p) dp \quad (9)$$

At the transition pressure, the thermodynamic equilibrium between the two phases $\Omega_{\text{os}}^{(1)}(P_{\text{eq}}) = \Omega_{\text{os}}^{(2)}(P_{\text{eq}})$ and thus $\Delta F_{\text{host}} = f_1(P_{\text{eq}}) - f_2(P_{\text{eq}})$.

It is clear that this method is straightforward to extend to cases where more than two solid phases come

into play, simply by applying the above construction to each structural transition. It is also worth noting that, if sorption isotherms are available for different temperatures, both energy and entropy differences, ΔU_{host} and ΔS_{host} , can be extracted from the free energies: $\Delta F_{\text{host}}(T) = \Delta U_{\text{host}} - T\Delta S_{\text{host}}$.

Taxonomy of guest-induced transitions in flexible frameworks

In this section, we apply the equations described above to the case of a nanoporous, flexible material that has two different metastable phases, and for which fluid adsorption follows type I isotherms in each structure. This case, including the possibility of one structure having no microporosity at all, has frequently been observed for hybrid organic–inorganic frameworks. We will show that this case yields a straightforward analytical expression for $\Delta\Omega_{\text{os}}(P)$ and enables us to propose a phenomenology of guest-induced structural transitions induced by adsorption and a classification of the resulting isotherms into distinct categories.

Let us consider that, for each phase i of the material, the adsorption happens in the gas phase (considered ideal) and follows a type I isotherm.²⁵ In order to keep the analytical expressions simple and to include only a few key physical quantities, the Langmuir equation is used to describe the gas adsorption:

$$N_{\text{ads}}^{(i)} = \frac{K_i P}{1 + \frac{K_i P}{N_{\text{max}}^i}} \quad (10)$$

where K_i is the Henry constant for adsorption, which measures the adsorption affinity, and N_{max}^i is the number of adsorbed gas molecules at the plateau of the isotherm. Plugging Equation 10 into Equation 8, and taking for V_{m} the expression of the ideal gas, the osmotic potential of phase i can be written as follows:

$$\Omega_{\text{os}}^{(i)} = F_{\text{host}}^{(i)} + PV_i - \int_0^P \frac{K_i}{1 + \frac{K_i P}{N_{\text{max}}^i}} dP = F_{\text{host}}^{(i)} + PV_i - N_{\text{max}}^i RT \ln \left(1 + \frac{K_i P}{N_{\text{max}}^i} \right) \quad (11)$$

The guest-induced structural transitions of the host material are dictated by the osmotic potentials $\Omega_{\text{os}}^{(i)}$ of the different solid phases as a function of pressure. We discuss in this section the conditions of occurrence of guest-induced transitions. We consider two structures of a single host material, labeled **1** and **2** in such a way that, in the absence of adsorbate, structure **1** is more stable than the structure **2** (i.e., $\Delta F_{\text{host}} = F_{\text{host}}^{(2)} - F_{\text{host}}^{(1)}$ is positive). The osmotic potential difference between these structures, as a function of pressure, is expressed as:

$$\Delta\Omega_{\text{os}} = \Delta F_{\text{host}} + P\Delta V - RT \left[N_{\text{max}}^{(2)} \ln \left(1 + \frac{K_2 P}{N_{\text{max}}^{(2)}} \right) - N_{\text{max}}^{(1)} \ln \left(1 + \frac{K_1 P}{N_{\text{max}}^{(1)}} \right) \right] \quad (12)$$

All the terms in this equation have a clear physical meaning and the full thermodynamic behavior can be discussed from there. To shorten the discussion, we now proceed to simplifying Equation 12. In all the cases presented in this article, gas adsorption happens in a range of pressures for which the term $P\Delta V$ in the expression above is of limited importance. To simplify the analytical formulas and the discussion that follows, $P\Delta V$ will thus be neglected in the rest of this section. Moreover, we replace the saturation values of the isotherms, N_{max}^i , with the accessible porous volume of the material in phase i , $V_{\text{p}}^{(i)}$, by writing $N_{\text{max}}^i = \rho V_{\text{p}}^{(i)}$, with ρ the density of the adsorbed gas at high pressure.⁴⁹

Equation 12 can then be rewritten as follows:

$$\Delta\Omega_{\text{os}}(P) = \Delta F_{\text{host}} - RT\rho \left[V_{\text{p}}^{(2)} \ln \left(1 + \frac{K_2 P}{\rho V_{\text{p}}^{(2)}} \right) - V_{\text{p}}^{(1)} \ln \left(1 + \frac{K_1 P}{\rho V_{\text{p}}^{(1)}} \right) \right] \quad (13)$$

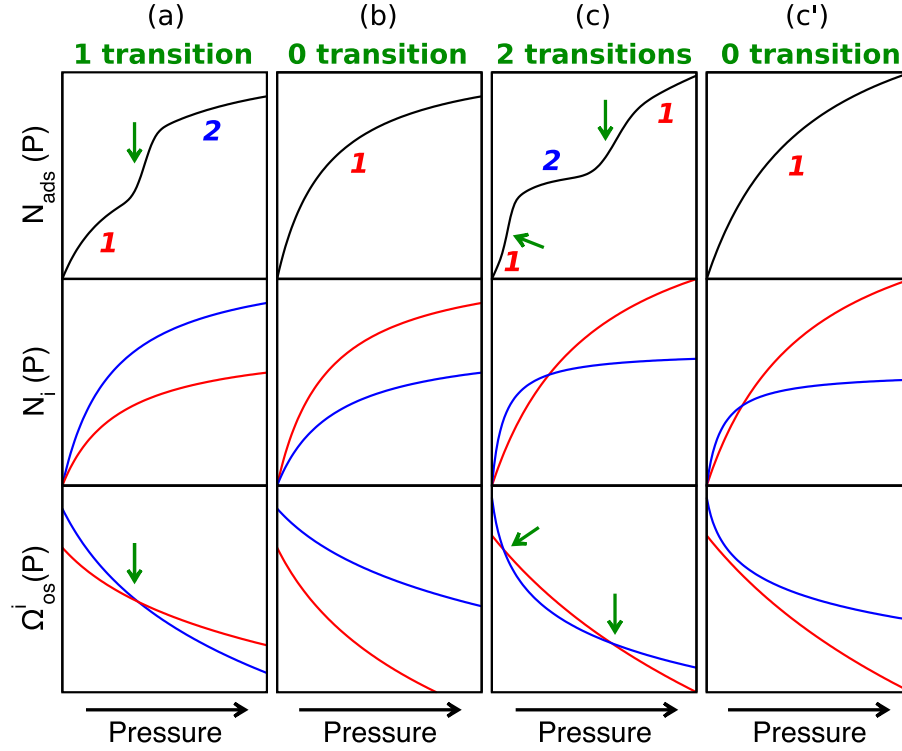


Figure 2: The four possible cases of Langmuir-type adsorption in materials with two metastable phases **1** and **2**. Top panels show the adsorption isotherms, middle panels depict the step-free isotherms corresponding to each phase, and bottom panels plot the osmotic potential of both phases. Green arrows indicate guest-induced structural transitions.

We now study the evolution of $\Delta\Omega_{\text{os}}(P)$ given by Equation 13 and in particular the solutions of the equation $\Delta\Omega_{\text{os}}(P) = 0$ (i.e., the structural transitions). As demonstrated in Appendix A, the behavior of the system and the occurrence of guest-induced phase transitions are entirely determined by five key parameters characteristic of the system: the difference in free energy between the empty host structures, ΔF_{host} , the pore volumes, $V_{\text{p}}^{(1)}$ and $V_{\text{p}}^{(2)}$, and the Henry constants, K_1 and K_2 . We can identify four distinct cases, synthesized in Figure 2:

- **Case a**, $V_{\text{p}}^{(2)} > V_{\text{p}}^{(1)}$: Under this condition, whatever the values of K_1 , K_2 and ΔF_{host} , only one structural transition is observed. Structure **1** will be more favorable at low pressure, and as pressure increases, the larger accessible pore volume of structure **2** will make it more and more favorable, leading to a structural transition upon adsorption.⁵⁰ This transition leads to a one-step isotherm (see Fig. 2, column **a**). This case is quite common and is actually observed in many of the so-called “third generation coordination polymers”¹³ that have attracted a lot of interest in the recent years. In the next section, we will show that our method can usefully be applied to two materials exhibiting crystal-to-crystal transformations of this type, including the example of $[\text{Cu}(4,4'\text{-bipy})(\text{dhbc})_2]$, and can apply to “gating processes”,³¹ where one of the structures has no microporosity at all.
- **Case b**, $V_{\text{p}}^{(1)} > V_{\text{p}}^{(2)}$ and $K_1 > K_2$: Under these conditions, we can predict that no structural transition will be observed. This stems from the fact that all factors favor structure **1**: the empty structure has lower free energy, it has higher adsorption affinity and higher pore volume (Fig. 2, column **b**).
- **Cases c and c'**, $V_{\text{p}}^{(1)} > V_{\text{p}}^{(2)}$ and $K_2 > K_1$: Under these conditions, two different behaviors must be dis-

tinguished. At low pressure, structure **1** is favored. At high pressure, it is also favored because it has a larger pore volume. In between, however, there might exist a regime where structure **2** is thermodynamically favored because of its larger adsorption affinity. Whether this regime occurs or not depends on the balance between the terms in Equation 13. If it happens, the system will undergo two successive structural transitions upon adsorption (from phase **1** to phase **2**, then back to phase **1**).

The condition for the occurrence of the double transition can be most easily expressed as an upper bound on the value of ΔF_{host} :

$$\frac{\Delta F_{\text{host}}}{\rho RT} < (V_2 - V_1) \ln \left(\frac{K_2 V_1 - K_1 V_2}{V_1 - V_2} \right) + V_1 \ln K_2 - V_2 \ln K_1 \quad (14)$$

Thus, if ΔF_{host} is small enough (or, seen the other way, if ΔK is large enough), there will be a domain of stability for structure **2**, and two transitions will be observed upon adsorption. This leads to an adsorption isotherm with two successive steps, as shown in third column of Fig. 2 (**case c**). On the other hand, if ΔF_{host} is too large (or ΔK too small), there will be no domain of stability for structure **2**, and structure **1** will be the most stable phase in the entire pressure range (see last column of Fig. 2, **case c'**), leading to the absence of structural transition. We will show later that the occurrence of a double guest-induced structural transition was indeed suggested experimentally in the case of CO₂ adsorption in MIL-53.^{35,51}

The cases considered above correspond to guest-induced transitions between two distinct host structures. More generally, this taxonomy can be extended to more complex cases where more than two host structures are involved.

Case studies of guest-induced transitions of hybrid frameworks

In this section, the above method is used to investigate the thermodynamics of three distinct cases of interest. The first one relates to the study of a recently discovered H₂-induced phase transition in a cobalt-based hybrid material. The second aims at studying the topical case of gate-opening processes. Finally, we will show how our method may be valuably applied to elucidate the thermodynamics of the rather complex case of the “breathing” of MOFs upon gas adsorption.

Structural phase transition in Co(1,4-benzenedipyrazolate) induced by H₂ adsorption

An interesting H₂ stepped isotherm was reported recently by Choi *et al.*, in the case of the Co(BDP) (BDP = 1,4-benzenedipyrazolate).²⁴ The area of hydrogen storage in hybrid materials is a particularly challenging and topical one,^{7,52} and any improvements in terms of H₂ storage capacity and performances are considered highly valuable. Until now, most hybrid frameworks had exhibited a traditional type I reversible H₂ adsorption isotherm, that allowed a ranking of the performances of materials on the sole basis of the weight adsorption capacity. By contrast, in the case of Co(BDP), the particular eye-catching feature is a stepped isotherm with a wide hysteresis,²⁴ allowing the adsorption of H₂ at high pressure and its storage at lower pressure,^{53,54} a highly desirable feature for practical applications such as transportation. The structural transition in Co(BDP) is reported to be induced by H₂ adsorption and therefore highlights that subtle energetic and thermodynamic effects are at play, having in mind that H₂ is associated with weak host-guest interactions in hybrid materials. This case caught our attention in the context of this work.

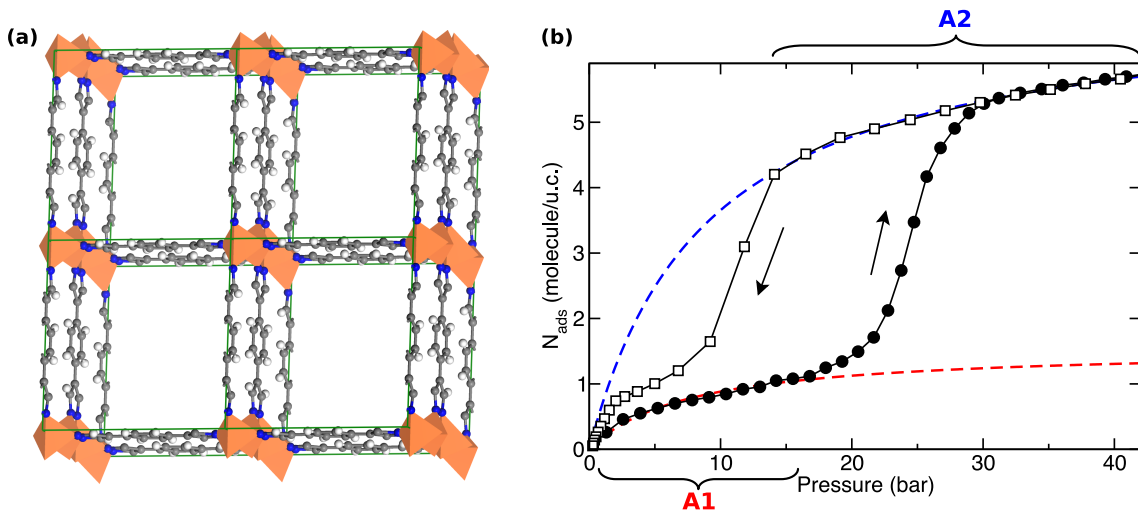


Figure 3: **(a)** $2 \times 2 \times 1$ supercell of structure **As**, $\text{Co}(\text{BDP}) \cdot 2\text{DEF} \cdot \text{H}_2\text{O}$, viewed along the c axis. **A2** is believed to have the same framework structure as **As**. **(b)** Adsorption and desorption isotherms, respectively in filled circles and empty squares, of H_2 in $\text{Co}(\text{BDP})$ at 77 K.²⁴ The blue dashed line is the fit of the upper part ($P \geq 15$ bar) of the desorption isotherm. The red dashed line is the fit of the lower part ($P \leq 15$ bar) of the adsorption isotherm.

The as-synthesized material $\text{Co}(\text{BDP}) \cdot 2\text{DEF} \cdot \text{H}_2\text{O}$ (DEF = N,N-diethylformamide), noted hereafter **As**, has a quadratic structure presenting $(10 \text{ \AA})^2$ square channels connected by narrow openings (see Figure 3a). Its full desolvation leads to the formation of crystalline $\text{Co}(\text{BDP})$, hereafter named **A1**, whose structure has not been solved; this process is reversible. N_2 adsorption in $\text{Co}(\text{BDP})$ at 77 K results in a multistep adsorption, interpreted by guest-induced transitions between **A1**, which has a rather small pore volume, and a fully open framework **A2**, believed to have the same framework structure as **As** on the basis of similarity of pore volume.

Experimental adsorption and desorption isotherms of H_2 in $\text{Co}(\text{BDP})$ were reported at 50 K, 65 K, 77 K and 87 K, showing various complex multisteped isotherms.²⁴ In this study, we have selected the isotherm at 77 K (Fig. 3b) because of its well-defined single-step isotherm, which was interpreted as resulting from a **A1**→**A2** structural transition. We apply here the method presented above to this experimental isotherm in order to calculate the free energy difference between **A1** and **A2**. The adsorption isotherm is fitted to a Langmuir equation in the 0–15 bar region to provide the “rigid-host” isotherm of phase **A1**; the desorption isotherm is fitted similarly in the 15–40 bar region to obtain the “rigid-host” isotherm of phase **A2**. Using the experimental isotherm, we estimate the thermodynamic transition to occur at $P_{\text{eq}} \approx 15$ bar, considering that the isotherm deviates from the Langmuir fits at 14 bar and 17 bar, for the desorption and adsorption branches respectively. Applying Equation 9 and neglecting the PV_i terms,⁵⁵ we find that the difference in free energy between **A1** and **A2** is of 3.3 kJ/mol (± 0.2 kJ/mol). This result is in very good agreement and much more accurate than the estimation put forth by Choi *et al.* that the energy of the structure change process lies in the 2–8 kJ/mol range.

It is interesting to note that this value of 3.3 kJ/mol, associated with an isotherm measured at 77 K, is significantly larger than the thermal energy kT (~ 5 times larger). Following the reasoning of Choi *et al.*, we can then use the calculated free energy difference between host phases to estimate the heat of adsorption of H_2 in $\text{Co}(\text{BDP})$, ΔH_{ads} , as $\Delta H_{\text{ads}} = \Delta H_{\text{host}} + \Delta_f H$. The latter term, $\Delta_f H$, is the formation enthalpy of a $\text{Co}(\text{BDP})\text{:H}_2$ clathrate complex and was estimated by Choi *et al.* to be 3.2 kJ/mol (± 0.3 kJ/mol). Neglecting entropic effects

at 77 K, this equation allows us to propose a heat of adsorption of ~ 6.5 kJ/mol for H_2 in $\text{Co}(\text{BDP})$. This heat of adsorption is rather in the lower region of the range typically observed, from 5 to 11 kJ/mol.⁵²

Gate-opening transition in a flexible coordination polymer

Gate-opening in flexible hybrid frameworks occurs when a material exhibit a structural transition from non-porous to porous structure at a specific pressure, and has been reported in a number of compounds.^{12,23,30,31} These materials are expected to find applications as sensors or switches, as well as gas separation. We focus here on the case of a particular flexible coordination polymer, $\text{Cu}(4,4'\text{-bipy})(\text{dhbc})_2 \cdot \text{H}_2\text{O}$ (4,4'-bipy = 4,4'-bipyridine; dhbc = 2,5-dihydroxybenzoate), whose as-synthesized structure **Bs** has been solved and which is known to exhibit a guest-induced structural transition upon adsorption of a large variety of gases (CO_2 , O_2 , CH_4 and N_2) at 298 K.³¹ The crystal-to-crystal structural transition occurs between two phases hereafter labeled **B1** and **B2**, whose structures have not been solved. **B1**, the dehydrated material, shows no microporosity and, upon gas adsorption, its channels open up at a given (guest-dependent) gate-opening pressure to yield the fully open **B2**. The framework structure of **B2** is the same as that of **Bs**, and is shown in Fig. 4a. It is composed of interdigitated two-dimension motifs (Fig. 4a, top) formed by copper (II) ions linked by bipyridine and dihydroxybenzoate linkers, and stacked due to π - π interactions between parallel dhbc ligands. Their interdigitation creates unidimensional channels along the a axis, with a 8 Å diameter.

The adsorption isotherms of various small molecules (N_2 , CH_4 and O_2 ; see Figure 4b) in structure **B1** at 298 K present common features: little to no adsorption in the lower pressure region, followed by a abrupt increase attributed to the **B1**→**B2** transition. Following Kaneko³⁰ and Kitagawa,³¹ we call here “gate-opening” pressure the point of the isotherm at which the structural transition happens during adsorption. The desorption isotherms, reversely, show an abrupt drop starting at a pressure that we will call the “gate-closing” pressure, where the **B2**→**B1** transition takes place. Each gate-closing pressure is lower than the corresponding gate-opening pressure, and the isotherms all exhibit hystereses. Only the isotherm for CO_2 is different in that transition happens at such a low pressure that no hysteresis was detected with the experimental setup.

We apply our method to each set of experimental isotherm (including CO_2) and calculate the difference in free energy between the two phases **B1** and **B2**. As structure **B1** is not porous, only the adsorption isotherm of structure **B2** is needed for the calculation. We use a Langmuir-type fit of the experimental desorption isotherms in the region of pressure higher than the gate-closing pressure. The fits, shown as dashed line for each isotherm in Fig. 4b, are all quite satisfactory. However, because the pressure of the thermodynamic structural transition can only be bracketed by the gate-opening and gate-closing pressures, the method does not lead to a single value of ΔF_{host} but to a range of free energy difference between structures.

Table 1 presents the values of free energy obtained from the isotherms of each gas. In each case, we find that the nonporous structure is more stable than the open one by 4 kJ/mol (± 0.5 kJ/mol) at 298 K. It is striking that, using different gas adsorption isotherms exhibiting different gate-opening and gate-closing pressure ranges, we obtain such narrow and consistent ranges for the value of ΔF_{host} . This excellent agreement between all the values independently obtained validates our approach and is a strong sign of the robustness and reliability of the method presented in this article. Indeed, in the absence of structural characterization of the transition, we show that a unique mechanism is at play behind the seemingly different features of all four isotherms.

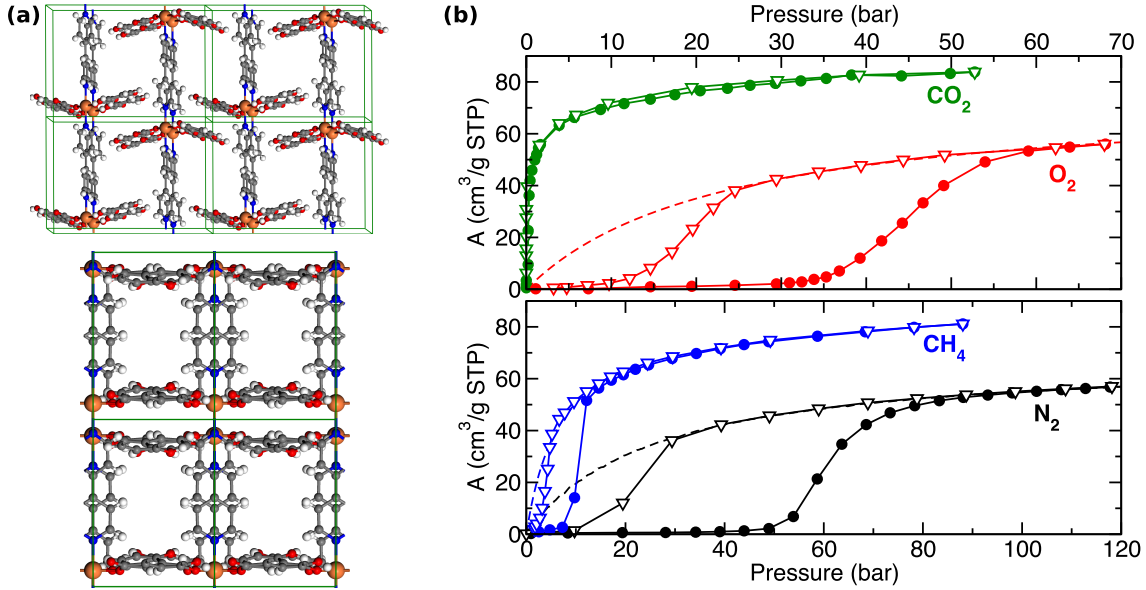


Figure 4: **(a)** 2×2 supercell of coordination polymer $[\text{Cu}(4,4'\text{-bipy})(\text{dhbc})_2] \cdot \text{H}_2\text{O}$: top, along the a axis; bottom, along the c axis. **(b)** Adsorption and desorption isotherms, respectively in filled circles and empty triangles, of various small molecules in $\text{Cu}(4,4'\text{-bipy})(\text{dhbc})_2$ at 298 K, as found in Ref. 31: CO_2 (green, upper panel), O_2 (red, upper panel), CH_4 (blue, lower panel) and N_2 (black, lower panel). The dashed lines are the fits of the upper part of each desorption isotherm (at pressure higher than the gate-closing pressure) by a Langmuir equation.

Adsorbate	Gate-opening	Gate-closing	Calculated ΔF_{host}
N_2	30 bar	49 bar	3.3 – 4.5 kJ/mol
CH_4	7 bar	12 bar	3.6 – 5.1 kJ/mol
O_2	25 bar	37 bar	3.4 – 4.3 kJ/mol
CO_2	< 2 bar	< 2 bar	< 6 kJ/mol

Table 1: Gate-opening and gate-closing pressures extracted from adsorption and desorption isotherms of various molecules in $[\text{Cu}(4,4'\text{-bipy})(\text{dhbc})_2] \cdot \text{H}_2\text{O}$, as well as free energy difference (at 298 K) between the open and closed structures of the material calculated from each isotherm; see text for details.

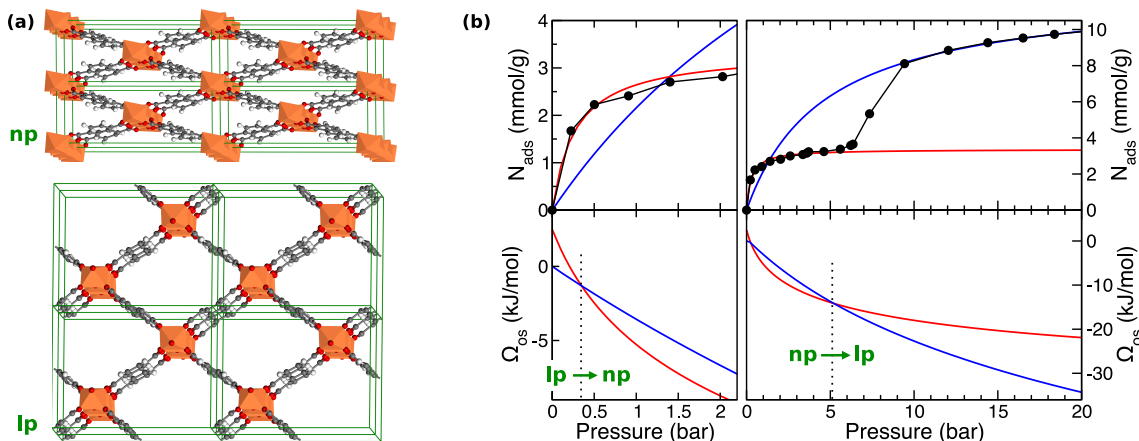


Figure 5: (a) Narrow-pore (**np**) and large-pore (**lp**) forms of the MIL-53 structure, viewed along the axis of the unidimensional channels. (b) Upper panel: experimental adsorption isotherm of CO₂ in MIL-53 (Al) at 304 K,⁵¹ as well as Langmuir fits of the 0–5 bar and 9–30 bar regions (in red and blue, respectively). Lower panel: osmotic thermodynamic potential as a function of CO₂ pressure for the **lp** (in blue) and **np** (in red) structures of MIL-53 (Al), calculated from the Langmuir fits.

“Breathing” phenomenon in the 3D hybrid framework MIL-53

The metal–organic framework MIL-53 has attracted a lot of attention due to the massive flexibility it exhibits, including structural characterization,^{32,35} adsorption of strategic gases H₂, CO₂ and CH₄^{51,56} and simulations.^{36,37,57} The MIL-53 framework topology is formed of unidimensional chains of corner-sharing MO₄(OH)₂ octahedra (M=Al³⁺, Cr³⁺) linked by 1,4-benzenedicarboxylate (BDC) ligands, which results in linear lozenge-shaped channels large enough to accommodate small guest molecules. This structure may oscillate between two distinct states, a large pore form (**lp**) and a narrow pore form (**np**), upon adsorption and desorption of gases; there is a $\sim 38\%$ difference in cell volume between these two forms. Both structures are depicted in Figure 5a.

The adsorption isotherm of CO₂ in MIL-53 at 304 K exhibit a step at approximately 6 bar (upper panel of Figure 5b), demonstrated to emanate from a structural transition upon adsorption from the CO₂-loaded **np** form to the CO₂-loaded **lp** one.³⁵ Moreover, as the most favorable guest-free MIL-53 is the large pore form at room temperature, another transition, **lp**→**np**, is expected at low pressure. Although it was not seen in the original adsorption isotherm,⁵¹ this low pressure transition was very recently confirmed by a combined simulation and microcalorimetry study.³⁶

Recently, a lot of effort has been put into understanding the energetics of these two guest-induced structural transitions, by Density Functional Theory³⁷ and forcefield-based calculations using rigid⁵⁷ or flexible³⁶ MIL-53 structures. Here, we bring the discussion one step further by giving valuable insight on the thermodynamics of this guest-induced structural transition using our method and the simple model developed above, yielding quantitative information on the relative stability of the two MIL-53 structures, which are virtually impenetrable experimentally.

The upper panel of Figure 5b shows the experimental adsorption isotherm of CO₂ in MIL-53 (Al). The step between 5 and 9 bar is a signature of the transition between the two phases of MIL-53 (Al), separating the part of the isotherm that corresponds to the **np** structure ($P < 5$ bar) and the part where the structure is fully open ($P > 9$ bar). Both parts were satisfactorily fitted by Langmuir isotherms (Fig. 5b) and Henry constants were

extracted (they are the slopes of the Langmuir fits at $P = 0$). The latter show clearly that the adsorption affinity of CO_2 is much higher in the **np** structure than in the **lp** one (3.5 times higher; $K_{\text{np}} \simeq 9.0 \times 10^{-5} \text{ mol kg}^{-1} \text{ Pa}^{-1}$ and $K_{\text{lp}} \simeq 2.6 \times 10^{-5} \text{ mol kg}^{-1} \text{ Pa}^{-1}$), in line with the energetics published so far.^{36,37,51} Indeed, with such features, MIL-53 exactly fits in *case c* of our taxonomy: the **lp** form is more stable in the absence of adsorbate and has a larger pore volume, but has a smaller affinity for CO_2 than **np**. Thus, according to our model, MIL-53 is expected to exhibit a double structural transition upon gas adsorption if the affinity is high enough: when empty and at very low pressure, the **lp** structure is intrinsically more stable; when pressure increases, the high affinity of the **np** structure leads to a **lp**→**np** transition; upon further rise of gas pressure, the larger pore volume of the open structure makes it favorable again and a **np**→**lp** transition should be observed. Our simple model predicts that, for this type I adsorption of gas in MIL-53 (Al, Cr), there is either no structural transition or two of them, depending on the nature of the gas. In the case of CO_2 , the experimental observation of one transition leads to the conclusion that another one must exist, at lower pressure, which was indeed recently evidenced.³⁶ By contrast, CH_4 has a much smaller adsorption affinity in MIL-53 and appears not to induce any structural transition,⁵¹ in agreement with our discussion above. These results highlight the correctness of the model and its ability to predict the occurrence or the absence of structural transitions for a given adsorbate, on the sole basis of its respective affinities for the host structures.

To quantify the effects discussed above, we have calculated the thermodynamic osmotic potential, $\Omega_{\text{os}}(P)$, of the **lp** and **np** phases of MIL-53 (Al) as a function of CO_2 pressure using the Eq. 8 and the fitted isotherms described above. From the experimental isotherm, we assume the equilibrium pressure for the **np**→**lp** transition to be around 5 bar. We then find a difference in free energy between the two structures of $\Delta F_{\text{lp-np}} \simeq 2.5 \text{ kJ/mol}$ per unit cell. A similar value was obtained for the chromium-containing form of MIL-53. The osmotic potential profiles (Fig. 5b, lower panel) clearly confirm the existence of two structural transitions upon adsorption and predict the low pressure **lp**→**np** transition to happen at 0.3 bar. It is noteworthy that this predicted value of the transition pressure is in very good agreement with the experimental value of 0.25 bar found very recently by microcalorimetry,³⁶ which is once again indicative of the predictive quality of the method exposed here. It also helps explaining why this low pressure transition was not visible on the original adsorption isotherm.

Conclusions

This article focuses on the specific class of hybrid materials exhibiting guest-induced structural transitions upon gas adsorption. Studies in this rapidly growing field mainly revolve around the structural characterization of these systems, the determination of their adsorption properties and the microscopic understanding of the coupling between the framework and adsorbate, e.g. by atomistic simulations. Here, we expose a general thermodynamic framework for gas adsorption in flexible hybrid materials and put forward a taxonomy of guest-induced structural transitions. This allows us to predict the occurrence or the absence of transitions of the host on the sole basis of a few key parameters: pore volumes, adsorption affinities and relative free energies of the framework structures involved in the transitions. Conversely, we show that these relative free energies can be extracted from experimental stepped isotherms, therefore quantifying the energetics of the phase transitions, which are especially difficult to access experimentally, however vital to the fundamental understanding of these systems. The robustness of our thermodynamic approach is illustrated through the analysis of three distinct cases of guest-

induced transitions: the hysteretic H₂ adsorption in a cobalt-based 3D framework, the gate-opening process in an interdigitated coordination polymer and the guest-dependent “breathing” phenomenon of MIL-53. We show that the free energy differences between the host structures involved in these guest-induced transitions fall into the 2–6 kJ/mol range. To our knowledge, this is the first general thermodynamic framework successfully rationalizing the variety of behaviors reported for this class of materials. We believe this work should prove very useful to explore new guest-induced transitions and further complement the current experimental and simulation approaches in the field.

Acknowledgments

This work was supported by the EPSRC (Advanced Research Fellowship awarded to CMD) and the FP-6 – European funding STREP “DeSanns” (SES6-CT-2005-020133) and “SURMOF” (NMP4-CT-2006-032109).

Supporting Information Available

Calculation details for the derivation of the taxonomy (Appendix A).

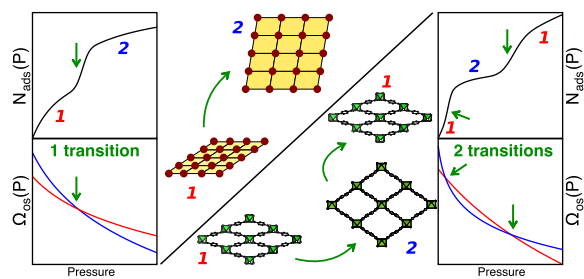
References

1. Kitagawa, S.; Kitaura, R.; Noro, S. *Angew. Chem. Int. Ed.* **2004**, *43*, 2334–2375.
2. Rosseinsky, M. J. *Microporous Mesoporous Mater.* **2004**, *73*, 15–30.
3. Cheetham, A. K.; Rao, C. N. R.; Feller, R. K. *Chem. Commun.* **2006**, 4780–4795.
4. Rao, C. N. R.; Cheetham, A. K.; Thirumurugan, A. *Journal of Physics: Condensed Matter* **2008**, *20*, 083202.
5. Férey, G.; Mellot-Draznieks, C.; Serre, C.; Millange, F. *Acc. Chem. Res.* **2005**, *38*, 217–225.
6. Kepert, C. K. *Chem. Commun.* **2006**, 695–700.
7. Rowsell, J. L. C.; Millward, A. R.; Park, K. S.; Yaghi, O. M. *J. Am. Chem. Soc.* **2004**, *126*, 5666–5667.
8. Latroche, M.; Surlblé, S.; Serre, C.; Mellot-Draznieks, C.; Llewellyn, P. L.; Lee, J.-H.; Chang, J.-S.; Jung, S. H.; Férey, G. *Angew. Chem. Int. Ed.* **2006**, *45*, 8227–8231.
9. Eddaoudi, M.; Kim, J.; Rosi, N.; Vodak, D.; Wachter, J.; O’Keeffe, M.; Yaghi, O. M. *Science* **2002**, *295*, 469–472.
10. Banerjee, R.; Phan, A.; Wang, B.; Knobler, C.; Furukawa, H.; O’Keeffe, M.; Yaghi, O. M. *Science* **2008**, *319*, 939–943.
11. Bradshaw, D.; Claridge, J. B.; Cussen, E. J.; Prior, T. J.; Rosseinsky, M. J. *Acc. Chem. Res.* **2005**, *38*, 273–282.
12. Fletcher, A. J.; Thomas, K. M.; Rosseinsky, M. J. *J. Solid State Chem.* **2005**, *178*, 2491–2510.
13. Kitagawa, S.; Uemura, K. *Chem. Soc. Rev.* **2005**, *34*, 109–119.
14. Uemura, K.; Matsuda, R.; Kitagawa, S. *J. Solid State Chem.* **2005**, *178*, 2420–2429.
15. Kondo, A.; Noguchi, H.; Carlucci, L.; Proserpio, D. M.; Ciani, G.; Kajiro, H.; Ohba, T.; Kanoh, H.; Kaneko, K. *J. Am. Chem. Soc.* **2007**, *129*, 12362–12362.
16. Noguchi, H.; Kondo, A.; Hattori, Y.; Kajiro, H.; Kanoh, H.; Kaneko, K. *J. Phys. Chem. C* **2007**, *111*, 248–254.
17. Maji, T. K.; Mostafa, G.; Matsuda, R.; Kitagawa, S. *J. Am. Chem. Soc.* **2005**, *127*, 17152–17153.
18. Chen, B.; Ma, S.; Hurtado, E. J.; Lobkovsky, E. B.; Liang, C.; Zhu, H.; Dai, S. *J. Phys. Chem. B* **2007**, *111*, 6101–6103.
19. Shimomura, S.; Horike, S.; Matsuda, R.; Kitagawa, S. *J. Am. Chem. Soc.* **2007**, *129*, 10990–10990.
20. Matsuda, R.; Kitaura, R.; Kitagawa, S.; Kubota, Y.; Belosludov, R. V.; Kobayashi, T. C.; Sakamoto, H.; Chiba, T.; Takata, M.; Kawazoe, Y.; Mita, Y. *Nature* **2005**, *436*, 238–241.
21. Goto, M.; Furukawa, M.; Miyamoto, J.; Kanoh, H.; Kaneko, K. *Langmuir* **2007**, *23*, 5264–5266.
22. Hu, S.; Zhang, J.-P.; Li, H.-X.; Tong, M.-L.; Chen, X.-M.; Kitagawa, S. *Cryst. Growth Des.* **2007**, *7*, 2286–2289.
23. Tanaka, D.; Nakagawa, K.; Higuchi, M.; Horike, S.; Kubota, Y.; Kobayashi, T. C.; Takata, M.; Kitagawa, S. *Angew. Chem. Int. Ed.* **2008**, *47*, 3914–3918.

24. Choi, H. J.; Dinca, M.; Long, J. R. *J. Am. Chem. Soc.* **2008**, *130*, 7848–7850.
25. Sing, K. S. W.; Everett, D. H.; Haul, R. A.; Moscou, L.; Pierotti, R. A.; Rouquerol, J.; Siemieniewska, T. *Pure Appl. Chem.* **1985**, *57*, 603–619.
26. Millward, A. R.; Yaghi, O. M. *J. Am. Chem. Soc.* **2005**, *127*, 17998–17999.
27. Walton, K. S.; Millward, A. R.; Dubbeldam, D.; Frost, H.; Low, J. J.; Yaghi, O. M.; Snurr, R. Q. *J. Am. Chem. Soc.* **2008**, *130*, 406–407.
28. Smit, B.; Maesen, T. L. M. *Nature* **2002**, *374*, 42–44.
29. Lachet, V.; Boutin, A.; Pellenq, R. J.-M.; Nicholson, D.; Fuchs, A. H. *J. Phys. Chem.* **1996**, *100*, 9006–9013.
30. Li, D.; Kaneko, K. *Chem. Phys. Lett.* **2001**, *335*, 50–56.
31. Kitaura, R.; Seki, K.; Akiyama, G.; Kitagawa, S. *Angew. Chem. Int. Ed.* **2003**, *42*, 428–431.
32. Serre, C.; Millange, F.; Thouvenot, C.; Nogues, M.; Marsolier, G.; Louër, D.; Férey, G. *J. Am. Chem. Soc.* **2002**, *124*, 13519–13526.
33. Mellot-Draznieks, C.; Serre, C.; Surblé, S.; Audebrand, N.; Férey, G. *J. Am. Chem. Soc.* **2005**, *127*, 16273–16278.
34. Serre, C.; Mellot-Draznieks, C.; Surblé, S.; Audebrand, N.; Filinchuk, Y.; Férey, G. *Science* **2007**, *315*, 1828–1831.
35. Serre, C.; Bourrelly, S.; Vimont, A.; Ramsahye, N. A.; Maurin, G.; Llewellyn, P. L.; Daturi, M.; Filinchuk, Y.; Leynaud, O.; Barnes, P.; G., F. *Adv. Mater.* **2007**, *19*, 2246–2251.
36. Coombes, D. S.; Bell, R.; Bourrelly, S.; Llewellyn, P. L.; Mellot-Draznieks, C., submitted for publication.
37. Ramsahye, N. A.; Maurin, G.; Bourrelly, S.; Llewellyn, P. L.; Serre, C.; Loiseau, T.; Devic, T.; Férey, G. *J. Phys. Chem. C* **2008**, *112*, 514–520.
38. Brennan, J. K.; Madden, W. G. *Macromolecules* **2002**, *35*, 2827–2834.
39. Banaszak, B. J.; Faller, R.; de Pablo, J. J. *J. Chem. Phys.* **2004**, *120*, 11304–11315.
40. Jeffroy, M.; Fuchs, A. H.; Boutin, A. *Chem. Commun.* **2008**, 3275–3277.
41. Snurr, R. Q.; Bell, A. T.; Theodorou, D. N. *J. Phys. Chem.* **1994**, *98*, 5111–5119.
42. Shen, J.; Monson, P. A. *Mol. Phys.* **2002**, *100*, 2031–2039.
43. Faure, F.; Rousseau, B.; Lachet, V.; Ungerer, P. *Fluid Phase Equilibria* **2007**, *261*, 168–175.
44. Peterson, B. K.; Gubbins, K. E. *Mol. Phys.* **1987**, *62*, 215–226.
45. Puibasset, J.; Pellenq, R. J. M. *J. Chem. Phys.* **2005**, *122*, 094704.
46. Cailliez, F.; Stirnemann, G.; Boutin, A.; Demachy, I.; Fuchs, A. H. *J. Phys. Chem. C* **2008**, *112*, 10435–10445.
47. Navrotsky, A. *Phys. Chem. Miner.* **1997**, *24*, 222–241.
48. The isotherm presented as illustration of the method has two parts that are each isotherms of type I, and thus appropriately fitted by Langmuir isotherms, but the method presented here is more general and can work as long as you have some *a priori* idea of the form of the isotherm and an adequate fitting function.

49. We assume that the fluid density in the pores at sufficiently high pressure is identical for all host phases, but the phenomenological discussion remains the same without this assumption, except that the pore volumes, $V_p^{(i)}$, are replaced by the saturation values of the isotherms, N_{\max}^i .
50. It is to be noted that, while the existence of this single transition is independent of the values of K_1 , K_2 and ΔF_{host} , the pressure at which it occurs is not: the smaller ΔF_{host} or the larger ΔK , the lower the transition pressure.
51. Bourrelly, S.; Llewellyn, P. L.; Serre, C.; Millange, F.; Loiseau, T.; Férey, G. *J. Am. Chem. Soc.* **2005**, *127*, 13519–13521.
52. Collins, D. J.; Zhou, H.-C. *J. Mater. Chem.* **2007**, *17*, 3154–3160.
53. Zhao, X.; Xiao, B.; Fletcher, A. J.; Thomas, K. M.; Bradshaw, D.; Rosseinsky, M. J. *Science* **2004**, *306*, 1012–1015.
54. Yang, C.; Wang, X.; Omary, M. A. *J. Am. Chem. Soc.* **2007**, *129*, 15454–15455.
55. We need to make this approximation because the unit cell parameters of structure **A1** are not known. It is justified by the fact that, as mentioned earlier, these terms have little influence in the range of pressure considered here. .
56. Férey, G.; Latroche, M.; Serre, C.; Millange, F.; Loiseau, T.; Percheron-Guegan, A. *Chem. Commun.* **2003**, 2976–2977.
57. Ramsahye, N. A.; Maurin, G.; Bourrelly, S.; Llewellyn, P. L.; Loiseau, T.; Serre, C.; Férey, G. *Chem. Comm.* **2007**, 3261–3263.

Table of Contents Graphic



Supplementary information for:

Thermodynamics of guest-induced structural transitions in hybrid organic–inorganic frameworks

F.-X. Coudert, M. Jeffroy, A.H. Fuchs, A. Boutin and C. Mellot-Draznieks

Appendix A: Calculation details

Starting with the expression of $\Delta\Omega_{\text{os}}(P)$ in Equation 13, we want to study the sign of $\Delta\Omega_{\text{os}}(P)$ and the solutions of the equation $\Delta\Omega_{\text{os}}(P) = 0$. To do so, we first compute the derivative of $\Delta\Omega_{\text{os}}(P)$ and we can show that:

$$\frac{d\Delta\Omega_{\text{os}}}{dP} = -\frac{\rho RT}{\left(\rho V_{\text{p}}^{(1)} + K_1 P\right) \left(\rho V_{\text{p}}^{(2)} + K_2 P\right)} \left(K_1 K_2 \Delta V_{\text{p}} P + \rho V_{\text{p}}^{(1)} V_{\text{p}}^{(2)} \Delta K\right)$$

The sign of the derivative is thus the same as that of $-\left(K_1 K_2 \Delta V_{\text{p}} P + \rho V_{\text{p}}^{(1)} V_{\text{p}}^{(2)} \Delta K\right)$. Four different cases need to be considered, depending on the sign of both ΔK and ΔV_{p} :

- If $\Delta V_{\text{p}} > 0$ and $\Delta K > 0$, the derivative will always be negative, and $\Delta\Omega_{\text{os}}(P)$ is strictly decreasing. As $\Delta\Omega_{\text{os}}(P = 0) = \Delta F_{\text{host}} > 0$, the equation $\Delta\Omega_{\text{os}}(P) = 0$ has one unique solution.
- If $\Delta V_{\text{p}} > 0$ and $\Delta K < 0$, the derivative will be positive around $P = 0$ and will become negative at higher pressure. $\Delta\Omega_{\text{os}}(P)$ has a positive value at $P = 0$, is first increasing, then decreasing; the equation $\Delta\Omega_{\text{os}}(P) = 0$ will once again have one solution (and only one).
- If $\Delta V_{\text{p}} < 0$ and $\Delta K < 0$, the derivative will always be positive and $\Delta\Omega_{\text{os}}(P)$ is increasing: at its value in $P = 0$ is positive, the equation $\Delta\Omega_{\text{os}}(P) = 0$ will have no solution.
- If $\Delta V_{\text{p}} < 0$ and $\Delta K > 0$, the derivative will be negative at small P and positive at larger P . Starting with a positive value at $P = 0$, $\Delta\Omega_{\text{os}}(P)$ will thus first decrease and then increase. Depending on the value it reaches at its minimum, the equation $\Delta\Omega_{\text{os}}(P) = 0$ will have zero, one (in the limiting case) or two solutions.

It is worth noting that the first two cases can be joined into a single case: if $\Delta V_{\text{p}} > 0$, the equation $\Delta\Omega_{\text{os}}(P) = 0$ has one unique solution.